Am J Physiol Renal Physiol 303: F632–F638, 2012.
First published June 13, 2012; doi:10.1152/ajprenal.00169.2012.

Flow-induced prostaglandin E_2 release regulates Na and K transport in the collecting duct

Daniel Flores,[1,2] Yu Liu,[1,2] Wen Liu,[3] Lisa M. Satlin,[1,3] and Rajeev Rohatgi[1,2,3]

[1]*Department of Medicine, The Mount Sinai School of Medicine,* [2]*Department of Medicine, The James J. Peters Veterans Affairs Medical Center,* [3]*Department of Pediatrics, The Mount Sinai School of Medicine, New York, New York*

Submitted 23 March 2012; accepted in final form 6 June 2012

Flores D, Liu Y, Liu W, Satlin LM, Rohatgi R. Flow-induced prostaglandin E_2 release regulates Na and K transport in the collecting duct. *Am J Physiol Renal Physiol* 303: F632–F638, 2012. First published June 13, 2012; doi:10.1152/ajprenal.00169.2012.—Fluid shear stress (FSS) is a critical regulator of cation transport in the collecting duct (CD). High-dietary sodium (Na) consumption increases urine flow, Na excretion, and prostaglandin E_2 (PGE_2) excretion. We hypothesize that increases in FSS elicited by increasing tubular flow rate induce the release of PGE_2 from renal epithelial cells into the extracellular compartment and regulate ion transport. Media retrieved from CD cells exposed to physiologic levels of FSS reveal several fold higher concentration of PGE_2 compared with static controls. Treatment of CD cells with either cyclooxygenase-1 (COX-1) or COX-2 inhibitors during exposure to FSS limited the increase in PGE_2 concentration to an equal extent, suggesting COX-1 and COX-2 contribute equally to FSS-induced PGE_2 release. Cytosolic phospholipase A2 (cPLA2), the principal enzyme that generates the COX substrate arachidonic acid, is regulated by mitogen-activated protein-kinase-dependent phosphorylation and intracellular Ca^{2+} concentration ($[Ca^{2+}]_i$), both signaling processes, of which, are activated by FSS. Inhibition of the ERK and p38 pathways reduced PGE_2 release by 53.3 ± 8.4 and 32.6 ± 11.3%, respectively, while antagonizing the JNK pathway had no effect. In addition, chelation of $[Ca^{2+}]_i$ limited the FSS-mediated increase in PGE_2 concentration by 47.5 ± 7.5% of that observed in untreated sheared cells. Sheared cells expressed greater phospho-cPLA2 protein abundance than static cells; however, COX-2 protein expression was unaffected ($P = 0.064$) by FSS. In microperfused CDs, COX inhibition enhanced flow-stimulated Na reabsorption and abolished flow-stimulated potassium (K) secretion, but did not affect ion transport at a slow flow rate, implicating that high tubular flow activates autocrine/paracrine PGE_2 release and, in turn, regulates flow-stimulated cation transport. In conclusion, FSS activates cPLA2 to generate PGE_2 that regulates flow-mediated Na and K transport in the native CD. We speculate that dietary sodium intake modulates tubular flow rate to regulate paracrine PGE_2 release and cation transport in the CD.

prostanoid; fluid shear stress; prostaglandin E_2; cyclooxygenase; cation transport

HIGH-SODIUM (HS) diets and attendant extracellular volume expansion induce intrarenal increases in prostaglandin (PG) synthesis, specifically PGE_2 (3, 17, 29, 31, 32). PGE_2 is an abundant renal PG and is a potent inhibitor of sodium (Na) and water reabsorption in the inner medullary collecting duct (IMCD) (20). Inhibition of PGE_2 synthesis is associated with avid renal Na absorption and hypertension, consistent with a critical role for PGE_2 in Na homeostasis and blood pressure regulation (29). Moreover, salt-sensitive hypertension is linked to deficiencies in renal PGE_2 synthesis and homeostasis (9, 12, 22). The physiologic and/or cellular triggers regulating PGE_2 synthesis and release in the CD that contribute to Na homeostasis are unknown.[1]

In murine models of HS intake, enzymes that synthesize PGE_2, including cyclooxygenase-1 (COX-1), COX-2, and microsomal prostaglandin E synthase-1 (mPGES-1), are increased (3). The mechanism underlying this response is unclear; however, alterations in urine tonicity have been implicated (30, 31). We hypothesized that fluid shear stress (FSS), accompanying high tubular flow rates elicited by HS feeding, triggers synthesis of PGE_2 and transcription/translation of the enzymes manufacturing PGE_2. To corroborate the physiologic relevance of FSS-induced changes in PGE_2 availability on cation transport, COX-dependent Na and potassium (K) transepithelial flux were measured in microperfused CDs under slow and fast flow rates.

MATERIALS AND METHODS

Cell culture. Murine immortalized IMCD3 or mpk cortical CD (mpkCCD) cells were grown in DMEM/F12 (with 10% fetal bovine serum) or DMEM:Ham's F12 (with 60 nM sodium selenate, 5 μg/ml transferrin, 2 mM glutamine, 50 nM dexamethasone, 1 nM tri-iodothyronine, 10 ng/ml epidermal growth factor, 5 μg/ml insulin, 20 mM D-glucose, 2% fetal calf serum, and 20 mM HEPES), respectively, on 25-mm × 75-mm slides or 40-mm glass coverslips and studied when they reached confluence between 3 and 7 days. We only used cells up to *passage 15* due to the risk of genetic drift.

Induction of FSS. Cells grown on slides and coverslips were placed in laminar flow chambers (Glycotech or Bioptechs manufactured chamber, respectively) and maintained at 37°C and subject to shear of 0.4 dyn/cm^2 using phenol red-free, serum-free DMEM/F12 containing penicillin/streptomycin for varying durations. FSS was calculated based on Poiseulle's law; $\tau = \mu\gamma = 6\mu Q/a^2b$ where τ = wall stress (dyn/cm^2), γ = shear rate (per s), μ = apparent viscosity of the fluid (media at 37°C = 0.76 cP), a = channel height (cm), b = channel width (cm), and Q = volumetric rate (ml/s). Static control cells were exposed to the same solution and duration as sheared cells, but without exposure to FSS. Cells from the Glycotech chamber were then collected for total RNA or protein while intracellular Ca^{2+} concentration ($[Ca^{2+}]_i$) was measured in cells placed in the Bioptechs chamber.

PGE_2 measurement. One milliliter of serum- and phenol red-free DMEM/F12 was incubated with either static or sheared cells for 1 h (19). The conditioned media were collected and frozen at −80°C for measurement of PGE_2 at a later time. PGE_2 concentration (pg/ml) was measured with a PGE_2 enzyme immunoassay kit (Cayman Chemical), following the standard protocol enclosed with the kit, and PGE_2 concentration was normalized to the amount of cellular protein to which the conditioned media were exposed. If sheared or static cells were exposed to the inhibitor, the inhibitor was also present in the conditioned media.

[1] This article is the topic of an Editorial Focus by Marcelo D. Carattino (2a).

Address for reprint requests and other correspondence: R. Rohatgi, One Gustave L. Levy Place, Box 1243, The Mount Sinai School of Medicine, New York, NY 10029 (e-mail: rajeev.rohatgi@mssm.edu).

Western blotting. Western blot analysis was performed as previously described (8). Cellular protein lysates (30 to 100 μg, depending on the abundance of the signal) were isolated as described above, resolved electrophoretically, and transferred to Immobilon filters (Millipore, Billerica, MA). Filters were blocked in 5% nonfat dried milk and 0.05% Tween and immunoblotted with a primary antibody (see *Reagents*). After being washed, blots were incubated with a horseradish peroxidase-conjugated secondary antibody (Sigma, St. Louis, MO) and bands were visualized by the West Pico enhanced chemiluminescence kit (Pierce, Rockford, IL). After the membrane was stripped and blocked, the blot was incubated with an anti-total-protein, anti-actin, or anti-glyceraldehyde-3-phosphate dehydrogenase (GAPDH)-specific antibody and visualized using the same methods as the primary antibody.

Quantitative real-time PCR. RNA was extracted from cells and cDNA was synthesized using random primers (27). Murine GAPDH was chosen as the internal positive reference control. qRT-PCR was performed as follows. In a 384-well plate, 0.2-μl cDNA sample was added plus 8 μl of a cocktail mix containing 0.05 μl Platinum *Taq* DNA Polymerase, 1 μl of 10× PCR buffer, 1.1 μl of 50 mM magnesium chloride, 0.1 μl AmpErase uracil *N*-glycosylase (UNG), 0.2 μl Gene Amp dNTPs with dUTP, 0.2 μl passive reference ROX dye, 0.2 μl (20 pM) forward and reverse primers, and 0.04 μl *Taq*man probe. *Taq* DNA Polymerase and ROX were purchased from Invitrogen (Carslbad, CA) and AmpErase UNG and dNTPs with dUTP from Applied Biosystems (Foster City, CA). Nuclease-free water was added for a total volume of 10 μl. Each plate was then covered with optical adhesive film and, after the initial steps of 50°C/2 min and 95°C/10 min, 40 cycles of 95°C/15 s (melt) and 60°C/1 min (anneal/extend), detection was performed in an ABI Prism 7900HT using SDS 2.2.1, Sequence Detection System software.

Measurement of $[Ca^{2+}]_i$. IMCD3 cells grown on 40-mm glass coverslips were incubated in serum-free DMEM/F12 media containing 25 μM FURA-2AM (Molecular Probes, Eugene, OR), a cell-permeant Ca^{2+} indicator dye, for 20 min. The cells were placed in a parallel plate-type laminar perfusion chamber (FCS2, Bioptechs, Butler, PA) and set on the stage of a Nikon Eclipse TE300 inverted epifluorescence microscope linked to a cooled Pentamax CCD camera (Princeton Instruments) interfaced with a digital imaging system (MetaFluor, Universal Imaging, Westchester, PA). The chamber temperature was maintained at 37°C with an FCS2 Temperature Controller (Bioptechs) and perfused using a FCS Micro-Perfusion Pump (Bioptechs). The shear generated across the monolayer was calculated using Poiseulle's law, as described above.

Cells in the laminar flow chamber were maintained in serum- and phenol red-free DMEM/F12 under no shear to confirm that baseline $[Ca^{2+}]_i$ was stable for 5 min. The pump rate was then abruptly increased to produce a shear of 0.4 dyn/cm^2 for ~10 min.

Throughout the experiment, cells were alternately excited at 340 and 380 nm and images, acquired every 1 to 15 s, were digitized for subsequent analysis. At the conclusion of each experiment, an intracellular Ca^{2+} calibration was performed using standard techniques (16). Standard equations were used to calculate experimental values of $[Ca^{2+}]_i$ for the cells monitored. Eight to eleven centrally located cells were analyzed in each monolayer per experiment. The mean baseline $[Ca^{2+}]_i$ value for each cell was calculated by averaging the eight $[Ca^{2+}]_i$ values measured just before increasing shear. The peak $[Ca^{2+}]_i$ was taken as the average of the three highest $[Ca^{2+}]_i$ values after induction of FSS.

Animals. Adult female New Zealand White rabbits were obtained from Covance (Denver, PA) and housed at the Mount Sinai School of Medicine Center for Comparative Medicine and Surgery. Animals were placed on a HS diet (Na^+: 140 meq/kg; K^+: 275 meq/kg) for 7–12 days and allowed free access to tap water. The HS diet was obtained from Harlan Teklad (Madison, WI). Animal weights and the amount of food and water consumed were monitored daily. All protocols were approved by the Institutional Animal Care and Use Committee of the Mount Sinai School of Medicine. Animals were euthanized in accordance with the National Institutes of Health *Guide for the Care and Use of Laboratory Animals*.

Microperfusion of single tubules. Kidneys were removed via a midline incision, and single cortical CDs (CCDs) were dissected in cold (4°C) Ringer solution and microperfused in vitro as previously described (5). Briefly, each isolated tubule was immediately transferred to a temperature- and O_2/CO_2-controlled specimen chamber, mounted on concentric glass pipettes, and perfused and bathed at 37°C with Burg's perfusate containing (in mM) 120 NaCl, 25 $NaHCO_3$, 2.5 K_2HPO_4, 2.0 $CaCl_2$, 1.2 $MgSO_4$, 4.0 Na lactate, 1.0 Na_3 citrate, 6.0 L-alanine, and 5.5 D-glucose, pH 7.4, 290 ± 2 mosmol/kgH_2O (5). During the 45-min equilibration period and thereafter, the perfusion chamber was continuously suffused with a gas mixture of 95% O_2-5% CO_2 to maintain the pH of the Burg's solution at 7.4 at 37°C. The bathing solution was continuously exchanged at a rate of 10 ml/h with a syringe pump (Razel, Stamford, CT).

Transport measurements were performed in the absence of transepithelial osmotic gradients, and thus water transport was assumed to be zero. Three or four samples of tubular fluid were collected under water-saturated light mineral oil by timed filling of a calibrated 30-nl volumetric constriction pipette at slow (~1 nl·min^{-1}·mm^{-1}) and fast (~5 nl·min^{-1}·mm^{-1}) flow rates. Indomethacin was added to the tubule during exposure to slow flow conditions. The K and Na concentrations of perfusate (C_0) and collected tubular fluid (C_L) were determined by helium glow photometry. The rates of K and Na transport (J_x; in pmol·min^{-1}·mm^{-1}) were calculated as follows: $J = (C_0 - C_L) \times V_L/L$, where V_L is the rate of collection of tubular fluid determined from the time (in min) required to fill the precalibrated volumetric pipette and L is the tubule length in millimeters. To determine the concentration of Na and K delivered to the tubular lumen, ouabain (100 μM) was added to the bath at the conclusion of each experiment to inhibit all active transport, and an additional three or four samples of tubular fluid were obtained for analysis. The rates of net transport (in pmol·min^{-1}·mm tubular length^{-1}) were calculated with standard flux equations, and the calculated ion fluxes were averaged to obtain a mean rate of ion transport for the CCD at each flow rate, as previously described (5). The flow rate was varied by adjusting the height of the perfusate reservoir. The sequence of flow rates was randomized within each group of tubules to minimize any bias induced by time-dependent changes in ion transport.

Reagents. Inhibitors were as follows: 10 μM U0126 (Calbiochem, San Diego, CA), 10 μM SB203580 (Cayman Chemical), 30 μM SP600125 (2) (Calbiochem), 125 μM indomethacin (14) (Sigma), 20 μM BAPTA-AM (Invitrogen), 100 nM SC560 (Cayman Chemical), and 1 μM CAY10404 (Cayman Chemical). Primers for qRT-PCR (Applied Biosciences) were as follows: COX-1 (Mm00477214_m1), COX-2 (Mm00478374_m1), Ptges-1 (Mm00452105_m1), and GAPDH (Mm99999915_g1); and antibodies were as follows: polyclonal anti-phospho-Ser505-cPLA2 (1:500; Cell Signaling), polyclonal cPLA2 (1:500; Cell Signaling), rabbit polyclonal anti-phospho-p38 (1:1,000; Cell Signaling), rabbit polyclonal anti-COX-2 (1:1,000; Cayman Chemical), mouse monoclonal anti-actin (1:1,000; Cell Signaling), mouse monoclonal anti-GAPDH (1:4,000; Santa Cruz Biotechnology), and goat anti-rabbit conjugated to horseradish peroxidase (1:5,000; Sigma).

Statistics. Data are given as means ± SE (n = number of slides or CCDs). Statistical analyses were performed using unpaired t-tests (SigmaStat version 2.03; SPSS, San Rafael, CA) for cell culture experiments and between treated and untreated CCDs, and paired t-test before and after indomethacin treatment of CCDs.

RESULTS

Immortalized IMCD3 and mpkCCD cells were exposed to a FSS of 0.4 dyn/cm^2 or static conditions for 2 h. This level of FSS was chosen because previously we demonstrated that

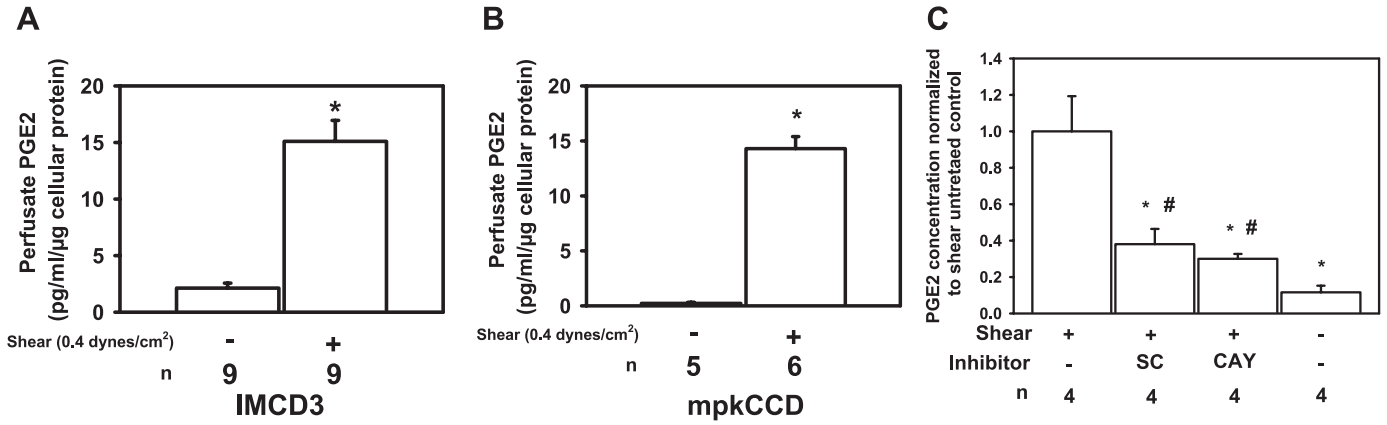

Fig. 1. Fluid shear stress (FSS) induces prostaglandin E_2 (PGE_2) secretion into the media bathing cultured inner medullary collecting duct type 3 (IMCD3; *A*) and mpk cortical collecting duct (mpkCCD; *B*) cells and this response in IMCD3 cells is inhibited equally by cyclooxygenase (COX)-1 or COX-2 inhibitors (*C*). IMCD3 and mpkCCD cells were grown to confluence and exposed to 0.4 dyn/cm^2 of FSS or maintained under static condition for 2 h. Cells were incubated in culture media for 1 h, the conditioned media were collected, and PGE_2 concentrations (pg/ml) were measured by enzyme immunoassay. The PGE_2 concentration was normalized to the amount of cellular protein ($pg \cdot ml^{-1} \cdot \mu g^{-1}$) present on the slide. Sheared IMCD3 (*A*) and mpkCCD (*B*) cells released more PGE_2 than their respective static controls. Inhibitors of COX-1 (100 nM SC560) or COX-2 (1 μM CAY10404) reduced FSS-induced PGE_2 release by 62.0 ± 8.4% ($*P < 0.05$) and 70.0 ± 2.7% ($*P < 0.05$) compared with the shear-untreated IMCD3 cells, respectively (*C*). PGE_2 concentration remained greater than static control ($\#P < 0.05$).

microperfused CCDs experience ~0.4–0.5 dyn/cm^2 of FSS when perfused at a fast physiologic flow rate (5 nl/min) (17). Conditioned media from shear-exposed IMCD3 cells expressed a greater concentration of PGE_2 per microgram of cellular protein than static controls (15.1 ± 1.9 vs. 2.1 ± 1.3 $pg \cdot ml^{-1} \cdot \mu g^{-1}$; Fig. 1*A*; $*P < 0.05$). An identical experiment in mpkCCD cells, a model of the CCD, found that the PGE_2 concentration was also greater in sheared than static controls (14.3 ± 1.1 vs. 0.2 ± 0.1 $pg \cdot ml^{-1} \cdot \mu g^{-1}$; Fig. 1*B*; $*P < 0.05$). Both CD cell lines exposed to FSS release PGE_2; however, we focused on IMCD3 cells because others have reported that immunodetectable PGE_2 synthetic enzymes, including COX-1/2 and mPGES-1, were upregulated in the renal medulla of mice fed a HS diet (3, 31, 32). To evaluate the contribution of COXs to FSS-induced PGE_2 release, sheared cells were treated with a COX-1 (SC560) or COX-2 (CAY10404) inhibitor and the FSS-induced increase in PGE_2 was measured in the perfusate (Fig. 1*C*). The inhibitor data are presented as percent reduction compared with untreated sheared cells. COX-1 and COX-2 inhibition attenuated the PGE_2 concentration in the media by 62.0 ± 8.4 and 70.0 ± 2.7% compared with untreated sheared cells (Fig. 1*C*; $*P < 0.05$), respectively, suggesting that both COX isoforms contribute equally to FSS-induced PGE_2 synthesis.

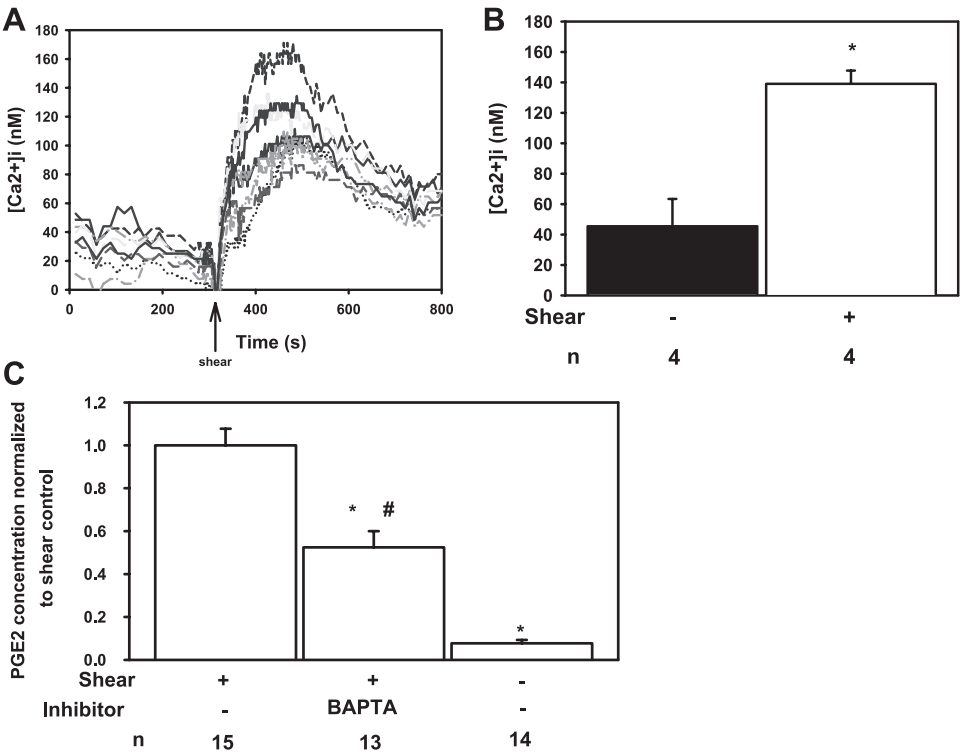

Fig. 2. FSS-mediated increase in intracellular Ca^{2+} concentration ($[Ca^{2+}]_i$) stimulates PGE_2 secretion. *A*: IMCD3 cells exposed to a sustained FSS of 0.4 dyn/cm^2 (arrow) experienced a rise in $[Ca^{2+}]_i$. *B*: peak $[Ca^{2+}]_i$ (139.0 ± 8.7 nM; $n = 4$; $*P < 0.05$) after exposure to FSS was greater than basal $[Ca^{2+}]_i$ under static conditions (45.4 ± 18.0 nM). *C*: treatment of IMCD3 cells with BAPTA-AM (20 μM) reduced FSS-induced PGE_2 secretion by 47.5 ± 7.5% compared with untreated sheared cells ($*P < 0.05$), but remained greater than static controls ($\#P < 0.05$).

Cytosolic phospholipase A2 (cPLA2) activity is regulated by two signaling pathways: *1*) increases in $[Ca^{2+}]_i$ (6, 11) and *2*) mitogen-activated protein (MAP)-kinase-dependent serine 505 phosphorylation of cPLA2 (11). Increases in $[Ca^{2+}]_i$ enhance translocation of cPLA2 to cellular membranes where it releases arachidonic acid (AA). cPLA2 activity is further augmented by MAP-kinase-dependent phosphorylation (13). Because FSS increases $[Ca^{2+}]_i$ (21, 28), ERK activity (8), and JNK activity (8) in CD epithelia, we hypothesized that FSS regulated PGE_2 release by activating cPLA2 through FSS-induced $[Ca^{2+}]_i$ changes and MAP-kinase activation.

To test this, we measured basal $[Ca^{2+}]_i$ under no flow and after exposure to FSS of 0.4 dyn/cm^2, as shown in Fig. 2*A*, a representative study. In the absence of FSS, $[Ca^{2+}]_i$ averaged 45.4 ± 18.0 nM, increasing to a peak of 139.0 ± 8.7 nM (Fig. 2*B*; $*P < 0.05$) after exposure to FSS. To test whether the FSS-induced increase in $[Ca^{2+}]_i$ is necessary for PGE_2 release, cells were pretreated with BAPTA-AM ($[Ca^{2+}]_i$ chelator) (15) and FSS-mediated PGE_2 concentration was measured in the media. BAPTA attenuated the FSS-induced increase in PGE_2 concentration in the media by 47.5 ± 7.5% of that observed in untreated sheared cells (Fig. 2*C*; $*P < 0.05$), but it remained greater than static controls ($\#P < 0.05$).

We previously demonstrated that FSS increased the abundance of phospho-ERK and phospho-JNK in IMCD3 cells so we next tested whether FSS induces the abundance of phospho-p38, also implicated in phosphorylating cPLA2 (8, 10). Phospho-p38 abundance was greater in sheared ($n = 4$) than static cells (Fig. 3*A*; $n = 5$, $P < 0.05$) at 120 min. To identify which MAP-kinases regulate FSS-induced release of PGE_2, sheared cells were incubated individually with U0126 (ERK pathway inhibitor), SB203580 (p38 pathway inhibitor), or SP600125 (JNK pathway inhibitor). U0126 and SB203580 reduced the PGE_2 concentration in the media by 53.3 ± 8.4 and 32.6 ± 11.3%, respectively, compared with shear-untreated controls (Fig. 3*B*; $*P < 0.05$) while SP600125 did not alter PGE_2 concentration (Fig. 3*B*), suggesting a role for ERK and p38 but not JNK in FSS-mediated PGE_2 release.

We then tested whether FSS activates cPLA2 by phosphorylating serine 505. Cells exposed to FSS for 120 min expressed greater steady-state abundance of phospho-cPLA2 than static cells (Fig. 4*A*), implicating the activation of cPLA2 and generation of AA in the FSS response. To test whether FSS alters the expression of the other genes involved in PGE_2 synthesis, the steady-state abundance of mRNAs encoding COX-1, COX-2, and mPGES-1 was measured in cells exposed to shear or static conditions. Expression of COX-1 and mPGES-1 mRNA was unaffected by FSS; however, COX-2 mRNA increased by 4.8 ± 0.9-fold compared with static cells (Fig. 4*B*; $*P < 0.05$). Next, lysates from cells exposed to FSS or static conditions for 2 h were immunoblotted with anti-COX-2 and anti-GAPDH antibodies and densitometric analysis was performed. In a single immunoblot (Fig. 4*C*), COX-2 protein appeared to be similar between sheared and static cells; however, in six experiments in total, COX-2 abundance tended to be greater in sheared (Fig. 4*D*, $n = 6$) than static ($n = 5$, $P = 0.064$) cells.

A HS diet induces CD COX gene and protein expression and urinary PGE_2 excretion while suppressing serum aldosterone to enhance Na excretion (3, 5). Estilo et al. (5) previously reported that flow-stimulated net Na absorption (J_{Na}) was

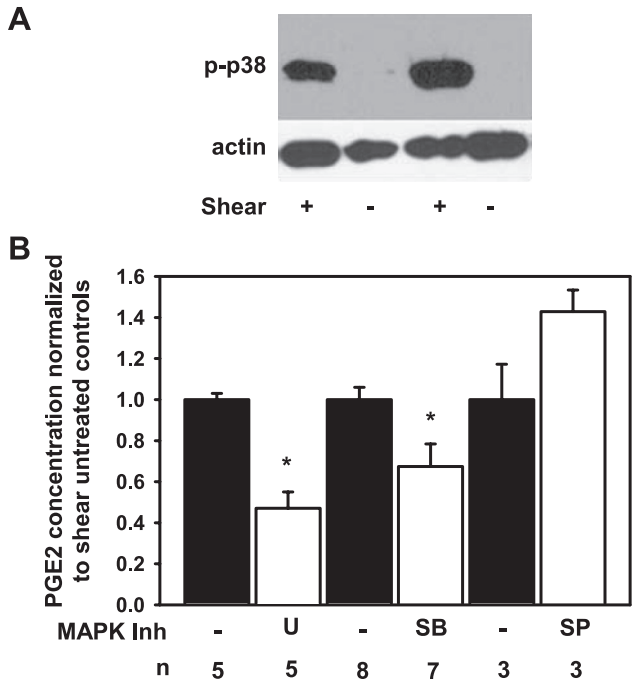

Fig. 3. FSS increases the abundance of phospho-p38 while inhibition of specific MAP kinase pathways reduces FSS-induced PGE_2 release. *A*: at 120 min, the steady-state abundance of phospho-p38 was greater in shear-exposed IMCD3 cells than static controls. *B*: IMCD3 cells were treated with ERK [10 μM U0126 (U)], p38 [10 μM SB203580 (SB)], and JNK [30 μM SP600125 (SP)] pathway inhibitors, exposed to 0.4 dyn/cm^2 of FSS for 2 h in the continuous presence of inhibitors, and PGE_2 concentration was measured in the media and normalized to the amount of cellular protein. The inhibitor data are presented as ratio to the shear-untreated controls (filled bars). U and SB reduced FSS-induced PGE_2 by 53.3 ± 8.4 and 32.6 ± 11.3%, respectively, compared with shear-untreated cells ($*P < 0.05$) while SP did not change PGE_2 secretion compared with shear-untreated control.

blunted in microperfused CCDs isolated from rabbits fed a HS diet when compared with transport rates measured in tubules from animals fed a low-Na diet (5). To test whether a flow-induced increase in PGE_2 synthesis/release in the CCD contributes to this blunted flow stimulation of J_{Na}, J_{Na} was measured in microperfused CCDs isolated from HS-fed rabbits before and after treatment with indomethacin. In a series of control untreated CCDs isolated from HS-fed rabbits, J_{Na} increased about threefold from 13.4 ± 3.9 to 38.8 ± 4.8 pmol·min^{-1}·mm^{-1} as the luminal flow rate was increased from a slow (~1) to a fast (5 nl·min^{-1}·mm^{-1}) flow rate (Fig. 5*A*, *left*; $*P < 0.05$); this increase in J_{Na} was similar to that observed by Estilo et al. (5) Addition of indomethacin to another set of CCDs perfused at slow flow rates had no significant effect on J_{Na} (16.2 ± 2.5 vs. 17.0 ± 1.5 pmol·min^{-1}·mm^{-1}). However, increasing the luminal flow rate in these indomethacin-treated CCDs to 5 nl·min^{-1}·mm^{-1} led to a greater than fourfold increase in J_{Na} to 63.2 ± 2.5 pmol·min^{-1}·mm^{-1} ($n = 4$; $@P < 0.05$). This rate of Na absorption was significantly greater than that measured in control untreated CCDs perfused at a similar fast flow rate ($\$P < 0.05$, via unpaired *t*-test). These data suggest that flow-stimulated PGE_2 synthesis/release in the CCD acts in an autocrine/paracrine fashion to blunt J_{Na} and that this repression of J_{Na} is abrogated when PGE_2 synthesis is inhibited by indomethacin. Measurement of net K secretion (J_K) in the

same CCDs described above showed that indomethacin (*right*) effectively blocked the typical flow-induced increase in J_K (-9.6 ± 2.4 to $-20.3+2.3$ pmol·min^{-1}·mm^{-1}; $^*P < 0.05$; Fig. 5*B*, *left*) observed in untreated control CCDs as luminal flow rate was increased from 1 to 5 nl·min^{-1}·mm^{-1} In CCDs perfused at a slow flow rate, J_K was similar in the absence and presence of indomethacin (-7.5 ± 1.8 to -7.0 ± 3.3 pmol·min^{-1}·mm^{-1}). However, in the presence of indomethacin flow-stimulated K secretion was abolished (-10.8 ± 3.4 pmol·min^{-1}·mm^{-1}; P = not significant vs. J_K in the same CCDs pefused at a slow flow rate).

In sum, inhibition of COX, and in particular PGE_2 synthesis, enhanced flow-stimulated J_{Na} and inhibited flow-induced J_K,

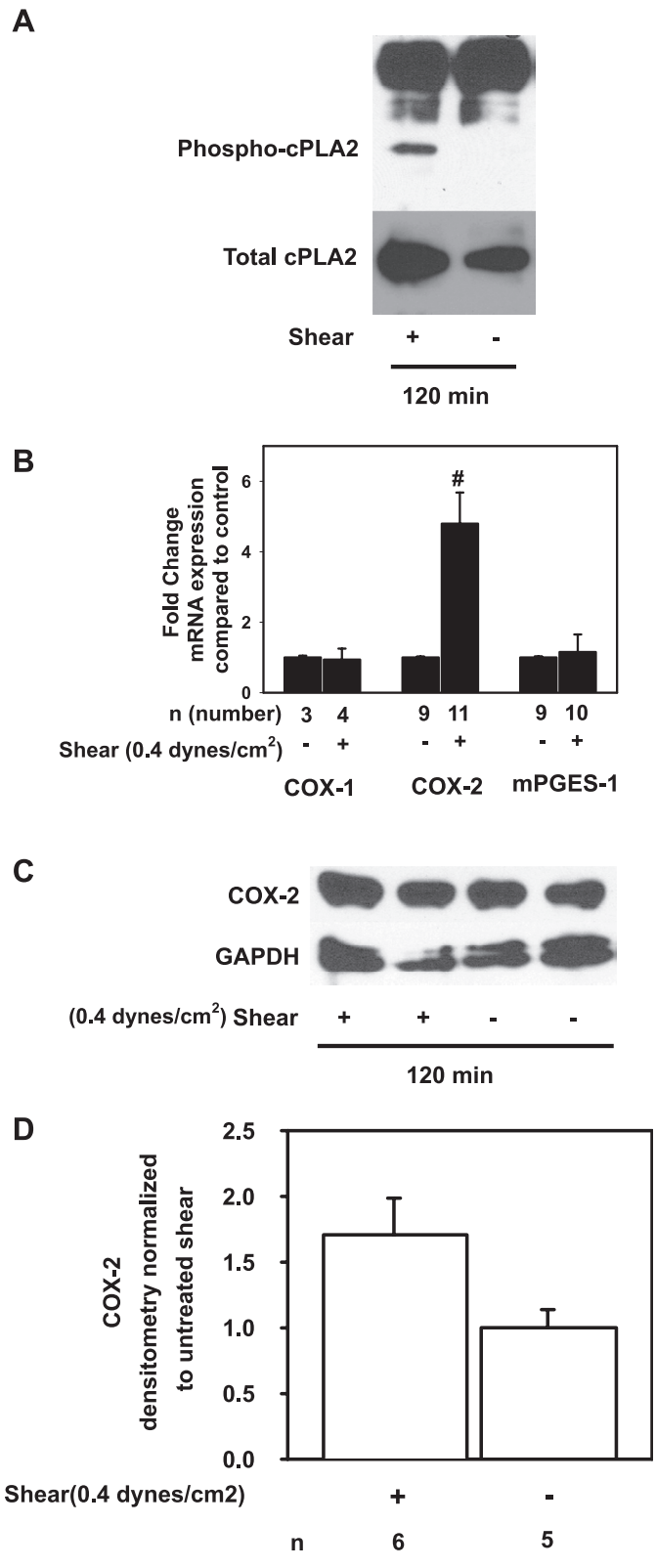

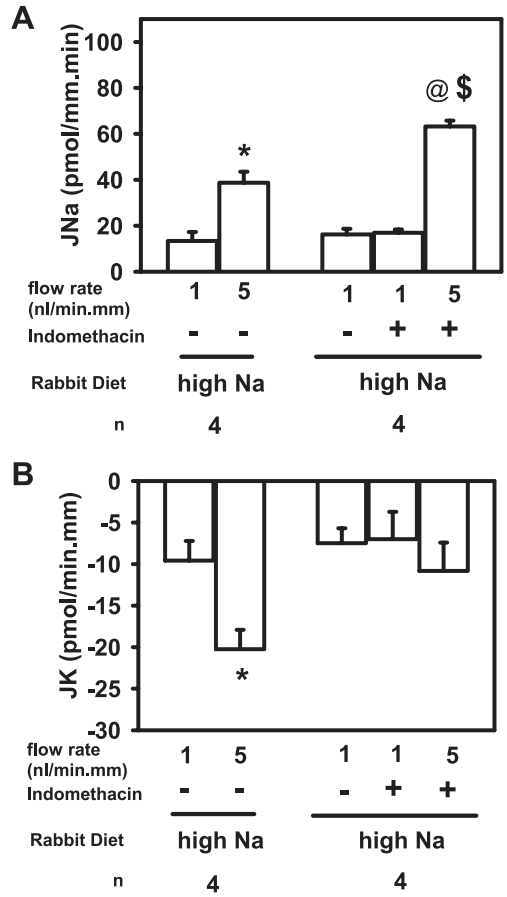

Fig. 5. Effect of COX inhibition (125 μM indomethacin) on net Na absorption (J_{Na}) and K secretion (J_K) in CCDs isolated from rabbits fed a high-salt (HS) diet. *A*, *left*: increase in tubular fluid flow rate from 1 (slow) to 5 (fast) nl·min^{-1}·mm^{-1} led to a 3-fold increase in J_{Na} ($n = 4$; $^*P < 0.05$). *A*, *right*: J_{Na} in CCDs perfused at a slow flow rate was unaffected by indomethacin. A 5-fold increase in luminal flow rate led to a >4-fold increase in J_{Na} ($@P < 0.05$, compared with J_{Na} measured in the same CCDs perfused at a slow flow; $\$P < 0.05$ vs. J_{Na} in untreated CCDs perfused at a similar fast flow rate). *B*, *left*: increase in tubular fluid flow rate from 1 to 5 nl·min^{-1}·mm^{-1} led to a 2-fold increase J_K ($n = 4$; $^*P < 0.05$). *B*, *right*: J_K in CCDs perfused at a slow flow rate was unaffected by indomethacin. However, indomethacin treatment abolished flow-induced K secretion.

Fig. 4. Phospho-cPLA2 abundance is increased in shear-exposed cells, but COX-1 and COX-2 gene and protein abundance are unaffected. *A*: IMCD3 cells exposed to 0.4 dyn/cm^2 of FSS for 2 h express high levels phospho-Ser505-cPLA2 while cells maintained under static conditions do not. *B*: COX-2 mRNA in shear-exposed cells increased by 4.8 ± 0.9-fold compared with static controls ($\#P < 0.05$) while COX-1 and mPGES-1 mRNA were unchanged. *C*: in a single experiment, COX-2 protein abundance was unaffected by 2 h of FSS. *D*: densitometric analysis of several experiments showed that there was a trend toward greater COX-2 protein abundance at 2 h ($P = 0.064$).

previously shown to reflect activation of the BK channel, but was without effect on cation transport in CCDs isolated from HS-fed rabbits and perfused at slow flow rates (15, 26). These results suggest that PGE_2 synthesis, stimulated in the CCD perfused at high tubular fluid flow rates, inhibits Na absorption and activates BK channel-mediated K secretion (14).

DISCUSSION

Although biomechanical forces play important physiologic and pathophysiologic roles in the kidney (1, 4, 7, 18, 21, 25), our understanding of how biophysical forces influence cellular processes and signaling pathways is in its infancy. This paper focused on the effect of FSS on renal epithelial PGE_2 release and the local paracrine effects of PGE_2 on CD cation transport. We demonstrate FSS enhances *1*) PGE_2 release through $[Ca^{2+}]_i$ and MAP-kinase-dependent signaling; *2*) the abundance of phosphorylated serine 505 of cPLA, an activated form of cPLA2 that releases AA; and *3*) the steady-state abundance of COX-2 mRNA, although COX-2 protein abundance was not statistically different. Moreover, in the setting of a HS diet, flow-stimulated cation transport was regulated by flow-stimulated, COX-dependent PGE_2 synthesis/release, permitting the independent regulation of Na reabsorption and K secretion. Activation of this important system would, thus, permit urinary K secretion in the face of HS diet and low serum aldosterone, which is expected to blunt K secretion.

Other investigators showed that stretch also may activate the eicosanoid system though cPLA2. In primary cultures of rabbit proximal tubular epithelial cells, cyclical stretch activated ERK-dependent phosphorylation of cPLA2 to release AA (1), similar to our suspected model of FSS activation of PGE_2. Treatment with BAPTA-AM did not affect stretch-mediated AA release but chelation of extracellular Ca^{2+} abrogated the stretch response (1). On the other hand, BAPTA-AM in our FSS model reduced PGE_2 release by ~50%. These differences in response to BAPTA-AM may be related to differences in the "stretch" vs. "shear" signal that is generated by the mechanical force or simply to differences in epithelial cell type (proximal tubule vs. CD). Moreover, raising the tubular flow rate in microperfused tubules not only increases apical FSS, but it also leads to circumferential stretch of the CD epithelia (17) and from our current experiments we cannot quantify the contribution of stretch to PGE_2-mediated cation transport.

In sum, our data add to the body of evidence that tubular flow and its hydrodynamic equivalent FSS are a physiologic trigger that activates autocrine/paracrine signaling systems in the CD to modulate cation transport. Recent evidence points to flow-triggered secretion of ATP (24), endothelin-1 (18), and 11,12 epoxyeicosatrienoic acid (11, 12 EET) (23) in the paracrine regulation of Na and K transport in the CD. However, this study is the first to demonstrate that a flow-stimulated paracrine factor is able to dissociate flow-stimulated Na and K transport in a nephron segment responsible for the final regulation of Na and K homeostasis. Of note is that Sun et al. (23) demonstrated that flow-stimulated K secretion was dependent on flow-induced 11,12 EET synthesis. We speculate that flow activation of cPLA2 is the principal mechanism by which 11,12 EET is synthesized since AA is the substrate for CYP-epoxygenase 2C23. This may reflect a common mechanism in the CD epithelia, in that increases in tubular flow rate activate cPLA2 and AA generation which forms the common substrate necessary for prostanoid, epoxyeicosatrienoic acid, lipoxin, leukotriene, and thromboxane synthesis. In conclusion, FSS-stimulated activation of cPLA2 and downstream PGE_2 synthesis/release are critical regulators of cation transport in the CD, and FSS activation of cPLA2 may reflect a common mechanism by which to generate AA, a common substrate to generate many other eicosanoids.

ACKNOWLEDGMENTS

We gratefully acknowledge the technical assistance of Beth Zavilowitz. These data were presented, in part, as an oral presentation at the 2009 American Society of Nephrology Meeting in San Diego, CA.

GRANTS

This work was supported by the Department of Veterans Affairs Merit Review 1I01BX000388 (R. Rohatgi), Pilot and Feasibility Grant from the Hepato/Renal Fibrocystic Diseases Core Center (DK074038-R. Rohatgi), RO1 DK38470 (L. M. Satlin), and The Pittsburgh Center for Kidney Research (DK079307-L. M. Satlin).

DISCLOSURES

No conflicts of interest, financial or otherwise, are declared by the author(s).

AUTHOR CONTRIBUTIONS

Author contributions: D.F., Y.L., W.L., and R.R. performed experiments; D.F. and L.M.S. interpreted results of experiments; D.F. prepared figures; L.M.S. edited and revised manuscript; R.R. conception and design of research; R.R. analyzed data; R.R. drafted manuscript.

REFERENCES

1. **Alexander LD, Alagarsamy S, Douglas JG.** Cyclic stretch-induced cPLA2 mediates ERK 1/2 signaling in rabbit proximal tubule cells. *Kidney Int* 65: 551–563, 2004.
2. **Bennett BL, Sasaki DT, Murray BW, O'Leary EC, Sakata ST, Xu W, Leisten JC, Motiwala A, Pierce S, Satoh Y, Bhagwat SS, Manning AM, Anderson DW.** SP600125, an anthrapyrazolone inhibitor of Jun N-terminal kinase. *Proc Natl Acad Sci USA* 98: 13681–13686, 2001.

2a. **Carattino MD.** *Cation transport goes with the flow*. Focus on "Flow-induced prostaglandin E_2 release regulates Na and K transport in the collecting duct." *Am J Physiol Renal Physiol* (June 13, 2012). doi:10.1152/ajprenal.00169.2012.

3. **Chen J, Zhao M, He W, Milne GL, Howard JR, Morrow J, Hebert RL, Breyer RM, Hao CM.** Increased dietary NaCl induces renal medullary PGE_2 production and natriuresis via the EP2 receptor. *Am J Physiol Renal Physiol* 295: F818–F825, 2008.
4. **Durvasula RV, Shankland SJ.** Mechanical strain increases SPARC levels in podocytes: implications for glomerulosclerosis. *Am J Physiol Renal Physiol* 289: F577–F584, 2005.
5. **Estilo G, Liu W, Pastor-Soler N, Mitchell P, Carattino MD, Kleyman TR, Satlin LM.** Effect of aldosterone on BK channel expression in mammalian cortical collecting duct. *Am J Physiol Renal Physiol* 295: F780–F788, 2008.
6. **Evans JH, Spencer DM, Zweifach A, Leslie CC.** Intracellular calcium signals regulating cytosolic phospholipase A2 translocation to internal membranes. *J Biol Chem* 276: 30150–30160, 2001.
7. **Faour WH, Thibodeau JF, Kennedy CR.** Mechanical stretch and prostaglandin E_2 modulate critical signaling pathways in mouse podocytes. *Cell Signal* 22: 1222–1230, 2010.
8. **Flores D, Battini L, Gusella GL, Rohatgi R.** Fluid shear stress induces renal epithelial gene expression through polycystin-2-dependent trafficking of extracellular regulated kinase. *Nephron Physiol* 117: p27–p36, 2010.
9. **Jia Z, Zhang A, Zhang H, Dong Z, Yang T.** Deletion of microsomal prostaglandin E synthase-1 increases sensitivity to salt loading and angiotensin II infusion. *Circ Res* 99: 1243–1251, 2006.
10. **Kramer RM, Roberts EF, Um SL, Borsch-Haubold AG, Watson SP, Fisher MJ, Jakubowski JA.** p38 mitogen-activated protein kinase phosphorylates cytosolic phospholipase A2 (cPLA2) in thrombin-stimulated platelets. Evidence that proline-directed phosphorylation is not required

for mobilization of arachidonic acid by cPLA2. *J Biol Chem* 271: 27723–27729, 1996.
11. **Leslie CC, Gangelhoff TA, Gelb MH.** Localization and function of cytosolic phospholipase A2alpha at the Golgi. *Biochimie* 92: 620–626, 2010.
12. **Limas C, Limas CJ.** Upregulation of renal prostaglandin receptors in genetic salt-dependent hypertension. *Hypertension* 8: 566–571, 1986.
13. **Lin LL, Wartmann M, Lin AY, Knopf JL, Seth A, Davis RJ.** cPLA2 is phosphorylated and activated by MAP kinase. *Cell* 72: 269–278, 1993.
14. **Ling BN, Webster CL, Eaton DC.** Eicosanoids modulate apical Ca^{2+}-dependent K^+ channels in cultured rabbit principal cells. *Am J Physiol Renal Fluid Electrolyte Physiol* 263: F116–F126, 1992.
15. **Liu W, Morimoto T, Woda C, Kleyman TR, Satlin LM.** Ca^{2+} dependence of flow-stimulated K secretion in the mammalian cortical collecting duct. *Am J Physiol Renal Physiol* 293: F227–F235, 2007.
16. **Liu W, Murcia NS, Duan Y, Weinbaum S, Yoder BK, Schwiebert E, Satlin LM.** Mechanoregulation of intracellular Ca^{2+} concentration is attenuated in collecting duct of monocilium-impaired orpk mice. *Am J Physiol Renal Physiol* 289: F978–F988, 2005.
17. **Liu W, Xu S, Woda C, Kim P, Weinbaum S, Satlin LM.** Effect of flow and stretch on the $[Ca^{2+}]_i$ response of principal and intercalated cells in cortical collecting duct. *Am J Physiol Renal Physiol* 285: F998–F1012, 2003.
18. **Lyon-Roberts B, Strait KA, van Peursem E, Kittikulsuth W, Pollock JS, Pollock DM, Kohan DE.** Flow regulation of collecting duct endothelin-1 production. *Am J Physiol Renal Physiol* 300: F650–F656, 2011.
19. **Malone AM, Anderson CT, Tummala P, Kwon RY, Johnston TR, Stearns T, Jacobs CR.** Primary cilia mediate mechanosensing in bone cells by a calcium-independent mechanism. *Proc Natl Acad Sci USA* 104: 13325–13330, 2007.
20. **Nasrallah R, Clark J, Hebert RL.** Prostaglandins in the kidney: developments since Y2K. *Clin Sci (Lond)* 113: 297–311, 2007.
21. **Nauli SM, Alenghat FJ, Luo Y, Williams E, Vassilev P, Li X, Elia AE, Lu W, Brown EM, Quinn SJ, Ingber DE, Zhou J.** Polycystins 1 and 2 mediate mechanosensation in the primary cilium of kidney cells. *Nat Genet* 33: 129–137, 2003.
22. **Reid GM, Appel RG, Dunn MJ.** Papillary collecting tubule synthesis of prostaglandin E2 in Dahl rats. *Hypertension* 11: 179–184, 1988.
23. **Sun P, Liu W, Lin DH, Yue P, Kemp R, Satlin LM, Wang WH.** Epoxyeicosatrienoic acid activates BK channels in the cortical collecting duct. *J Am Soc Nephrol* 20: 513–523, 2008.
24. **Vallon V, Rieg T.** Regulation of renal NaCl and water transport by the ATP/UTP/P2Y2 receptor system. *Am J Physiol Renal Physiol* 301: F463–F475, 2011.
25. **Weinbaum S, Duan Y, Satlin LM, Wang T, Weinstein AM.** Mechanotransduction in the renal tubule. *Am J Physiol Renal Physiol* 299: F1220–F1236, 2010.
26. **Woda CB, Bragin A, Kleyman TR, Satlin LM.** Flow-dependent K^+ secretion in the cortical collecting duct is mediated by a maxi-K channel. *Am J Physiol Renal Physiol* 280: F786–F793, 2001.
27. **Woda CB, Miyawaki N, Ramalakshmi S, Ramkumar M, Rojas R, Zavilowitz B, Kleyman TR, Satlin LM.** Ontogeny of flow-stimulated potassium secretion in rabbit cortical collecting duct: functional and molecular aspects. *Am J Physiol Renal Physiol* 285: F629–F639, 2003.
28. **Xu C, Rossetti S, Jiang L, Harris PC, Brown-Glaberman U, Wandinger-Ness A, Bacallao RL, Alper SL.** Human ADPKD primary cyst epithelial cells with a novel, single codon deletion in the PKD1 gene exhibit defective ciliary polycystin localization and loss of flow-induced Ca^{2+} signaling. *Am J Physiol Renal Physiol* 296: F1464–F1476, 2006.
29. **Yang T.** Microsomal prostaglandin E synthase-1 and blood pressure regulation. *Kidney Int* 72: 274–278, 2007.
30. **Yang T, Schnermann JB, Briggs JP.** Regulation of cyclooxygenase-2 expression in renal medulla by tonicity in vivo and in vitro. *Am J Physiol Renal Physiol* 277: F1–F9, 1999.
31. **Yang T, Singh I, Pham H, Sun D, Smart A, Schnermann JB, Briggs JP.** Regulation of cyclooxygenase expression in the kidney by dietary salt intake. *Am J Physiol Renal Physiol* 274: F481–F489, 1998.
32. **Ye W, Zhang H, Hillas E, Kohan DE, Miller RL, Nelson RD, Honeggar M, Yang T.** Expression and function of COX isoforms in renal medulla: evidence for regulation of salt sensitivity and blood pressure. *Am J Physiol Renal Physiol* 290: F542–F549, 2006.